TITLE:

Arabidopsis thaliana subclass I ACTIN DEPOLYMERIZING FACTORs regulate nuclear organization and gene expression

AUTHORS:

[1]Tomoko Matsumoto, [2,3]Takumi Higaki, [4]Hirotomo Takatsuka[†], [5]Natsumaro Kutsuna, [1]Yoshiyuki Ogata, [6]Seiichiro Hasezawa, [4]Masaaki Umeda and [1]Noriko Inada*

ADDRESS:

[1]Graduate School of Agriculture, Osaka Metropolitan University, 1-1 Gakuen-cho, Naka-ku, Sakai, Osaka 599-8531, Japan

[2]Graduate School of Science and Technology, Kumamoto University, Kumamoto 860-8555, Japan

[3]International Research Organization for Advanced Science and Technology (IROAST), Kumamoto University, Kumamoto 860-8555, Japan

[4]Graduate School of Science and Technology, Nara Institute of Science and Technology, Takayama-cho 8916-5 Ikoma, Nara 630-0192 Japan

[5]LPIXEL, Inc., 1-6-1 Otemachi, Chiyoda-ku, Tokyo 100-0004, Japan

[6]Graduate School of Science and Engineering, Hosei University, Tokyo 102-8160, Japan

[†]Present address:School of Biological Science and Technology, College of Science and Engineering, Kanazawa University, Kakuma-machi, Kanazawa 920-1192, Japan

*Author in correspondence

ABSTRACT

ACTIN DEPOLYMERIZING FACTOR (ADF) is a conserved protein that regulates the organization and dynamics of actin microfilaments. Eleven ADFs in the *Arabidopsis thaliana* genome are grouped into four subclasses, and subclass I ADFs, ADF1–4, are all expressed throughout the plant. Previously, we showed that subclass I ADFs function in the regulation of the response against powdery mildew fungus as well as in the regulation of cell size and endoreduplication. Here, we report a new role of subclass I ADFs in the regulation of nuclear organization and gene expression. Through a microscopic observation of epidermal cells in mature leaves, we found that the size of chromocenters in both *adf4* and transgenic lines where expression of subclass I *ADF*s are downregulated (*ADF1-4Ri*) was reduced compared with that of wild-type Col-0. *A. thaliana* possesses eight *ACTIN* genes, among which *ACT2*, *-7*, and *-8* are expressed in vegetative organs. The chromocenter size in *act7*, but not in the *act2/8* double mutant, was enlarged compared with that in Col-0. Microarray analysis revealed that 1,818 genes were differentially expressed in *adf4* and *ADF1-4Ri*. In particular, expression of 22 nucleotide-binding leucine-rich repeat (*NLR*) genes, which are involved in effector-triggered plant immunity, was reduced in *adf4* and *ADF1-4Ri*. qRT-PCR confirmed the altered expressions shown with microarray analysis. Overall, these results suggest that ADF regulates various aspects of plant physiology through its role in regulation of nuclear organization and gene expression. The mechanism how ADF and ACTIN regulate nuclear organization and gene expression is discussed.

INTRODUCTION

Actin depolymerizing factor (ADF) is an ancient protein that is conserved among eukaryotes. ADF regulates both the organization and dynamics of actin microfilaments (AFs) by severing these and depolymerizing them at the minus end (Inada, 2017). Analyses using various plants including *Arabidopsis thaliana* have revealed that ADFs function in regulating many aspects of plant physiology, including growth and development (Dong et al. 2001, Henty et al. 2011, Inada et al. 2021), flowering (Dong et al. 2001, Burgos-Rivera et al. 2008), immunity against bacterial (Tian et al. 2009, Porter et al. 2012) and fungal pathogens (Inada et al. 2016, Zhang et al. 2017, Sun et al. 2021), root-knot nematodes (Clément et al. 2009), and aphids (Mondal et al. 2018), rhizobial infection and nodule formation (Ortega-Ortega et al. 2020), and responses against drought (Qian et al. 2019, Sengupta et al. 2019), salt stress (Sengupta et al. 2019, Wang et al. 2021), and low temperature (Xu et al. 2021). However, it is unknown how ADFs regulate these broad aspects of plant physiology.

AFs mainly function underneath the plasma membrane by regulating intercellular transport (Henty-Ridilla et al. 2013); however, recent research using animal and insect cells has shown the roles of actin and actin-binding proteins in the nucleus and in the regulation of gene expression.

68 The actin monomer has been shown to be a functional component of RNA polymerases and
69 chromosome remodeling complex (Percipalle and Vartiainen 2019). Furthermore, recent
70 development of nuclear AF visualization method revealed that nuclear AFs are transiently
71 formed upon various stimuli, such as treatments with serum and reagents that induce DNA
72 damage (Baarlink et al. 2013, Hurst et al. 2019) and contribute to the regulation of gene
73 expression (Percipalle and Vartiainen 2019). Cytoplasmic AFs also regulate gene expression
74 through association with nuclear envelope-embedded protein complexes (Davidson and Cadot
75 2021).
76 Interest has increased in plants in the role of actin and actin-binding proteins in the nucleus
77 and in the regulation of gene expression (Porter and Day 2013, Porter and Day 2016, Inada
78 2017). Immunostaining using antibodies that label *A. thaliana* ACTIN2/8 (ACT2/8) and ACT7
79 showed accumulation of these actins within isolated nuclei (Kandasamy et al. 2010). Among the
80 11 members of ADFs in *A. thaliana* (Ruzicka et al. 2007, Inada, 2017), a knockout mutant of
81 *ADF4* showed an increased susceptibility against the bacterial pathogen *Pseudomonas syringae*
82 DC3000 harboring AvrPphB (Tian et al. 2009). This increased susceptibility is correlated with a
83 decreased expression of *FRK1* and *RPS5*, which encode bacterial flagellin-induced receptor
84 kinase and a resistance protein required for recognition of AvrPphB, respectively (Porter et al.
85 2012). The loss of *A. thaliana ADF9* expression causes reduced expression of *FLOWERING*
86 *LOCUS C* (*FLC*), which is a master repressor of the transition from the vegetative to
87 reproductive growth, and increased expression of *CONSTANS* (*CO*), *FLOWERING LOCUS T*
88 (*FT*), *SUPRESSOR OF CONSTANS1* (*SOC1*), and *LEAFY* (*LFY*), resulting in early flowering
89 (Burgos-Rivera et al. 2008).
90 We previously demonstrated that *A. thaliana* subclass I ADFs (ADF1-4), particularly
91 ADF4, are involved in response against powdery mildew fungus (Inada et al. 2016) as well as in
92 the regulation of endoreduplication and plant size (Inada et al. 2021) and suggested that subclass
93 I ADFs may have a function in the nucleus and in the regulation of gene expression. The *ADF4*-
94 knockout mutant showed strong resistance against the *A. thaliana*-adapted powdery mildew
95 fungus *Golovinomyces orontii*. This resistance was further enhanced in transgenic plants where
96 expression of all subclass I *ADF*s was suppressed (*ADF1-4Ri*). By visualizing AFs with
97 expression of GFP-hTalin (Takemoto et al. 2003), we found that the density and level of
98 bundling of AFs at the cell surface are not significantly altered in both *adf4* and *ADF1-4Ri*.
99 Observation of *adf4* plants expressing ADF4-GFP revealed nuclear localization of ADF4 in
100 addition to colocalization with AFs at the cell surface. Expression of ADF4-GFP complemented
101 the *adf4 G. orontii*-resistant phenotype. However, expression of ADF4-GFP conjugated with
102 nuclear exporting signal did not complement *adf4*, indicating that nuclear localization of ADF4
103 is important for response against *G. orontii* (Inada et al. 2016). We found that *adf4* and *ADF1-*
104 *4Ri* had an increased plant size and an enhanced endoreduplication (Inada et al. 2021). All
105 known factors that regulate endoreduplication are localized to the nucleus (discussed in Inada et
106 al. 2021), further suggesting the role of subclass I ADFs in the nucleus or in the regulation of
107 events occurring within the nucleus.

108 In this study, we characterized the nuclear morphology and gene expression profile of *A.*
109 *thaliana adf* mutants. Nuclei in epidermal cells of *A. thaliana* mature leaves contain distinctive
110 chromocenters that are strongly stained with DNA-binding fluorescent dyes (Fransz et al. 2002).
111 By a close observation using confocal laser scanning microscope, we found that the size of these
112 chromocenters of nuclei in the epidermal cells of mature leaves was significantly reduced in *adf4*
113 and *ADF1-4Ri* transgenic plants (Tian et al. 2009). The *A. thaliana* genome contains eight
114 ACTIN members, of which *ACTIN2*, -*7*, and -*8* are expressed in vegetative tissues (McKinney
115 and Meagher 1998). We found that *act7*, but not *act2/8* mutants showed increased chromocenter
116 size. Microarray analysis of wild-type Col-0, *adf4*, and *ADF1-4Ri* mature leaves showed that
117 expression of a large number of genes was altered in both *adf4* and *ADF1-4Ri*. These results
118 suggest that actin and ADF are involved in the regulation of nuclear organization and of gene
119 expression.
120
121
122 **RESULTS**
123
124 **The nuclear organization was altered in both *adf4* and *ADF1-4Ri***
125 For the first step to understand the role of ADFs in the nucleus or in the regulation of events
126 occurring in the nucleus, we took a close observation of nuclei using a confocal laser scanning
127 microscope. In fixed-*A. thaliana* mature leaves, 4′,6-diamidino-2-phenylindole (DAPI)-stained
128 nuclei contain well-defined chromocenters (Fransz et al. 2002). These chromocenters consist of
129 heterochromatin regions including centromeric and pericentromeric domains as well as nucleolar
130 organizing regions (NORs) that are composed of ribosomal DNA tandem repeats located in the
131 short arms of chromosomes 2 and 4 (Fransz et al. 2002). NORs are located close to the nucleolus
132 while centromeres are located near the nuclear periphery. By observing epidermal nuclei in
133 mature leaves, we noticed that chromocenters in both *adf4* and *ADF1-4Ri* were smaller than
134 those in Col-0 (Figs. 1A–C). No significant alteration in the shape and size of nuclei was noticed.
135 To quantify the size of chromocenters, maximum projection images produced from Z-stack
136 DAPI-stained nuclei images were processed to evaluate the chromocenter regions. The number
137 of chromocenters per nucleus (Fig. 1D), average size of nucleus (Fig. 1E), average size of
138 chromocenters (Fig. 1F), and percentage of area occupied by chromocenters in the nucleus (Fig.
139 1G) were determined. Wild-type Col-0 nuclei contain 8–10 chromocenters as in previous
140 observations (Fransz et al. 2002). As shown in Fig. 1D, the number of chromocenters per nucleus
141 was unaltered in *adf4* and *ADF1-4Ri*. The size of nuclei in *adf4* and *ADF1-4Ri* was comparable
142 with that in Col-0 (Fig. 1E). However, the average size of chromocenters in both *adf4* and
143 *ADF1-4Ri* was significantly reduced compared with that in Col-0 (Fig. 1F). The percentage of
144 chromocenter occupancy in the nucleus was also significantly reduced in *ADF1-4Ri* but not in
145 *adf4* (Fig. 1G). Four independent lines have been established for *ADF1-4Ri* (Tian et al. 2009),
146 and all *ADF1-4Ri* lines showed significant reduction in chromocenter size (Fig. S1).

147 Close examination of the obtained images showed that the NOR chromocenters tended to
148 be larger than those near the nuclear periphery in *adf4* and *ADF1-4Ri* (Figs. 1A–C; nucleoli are
149 indicated by dotted lines). We examined the size of NOR chromocenters separately from
150 chromocenters located at the nuclear periphery. The size of chromocenters at the nuclear
151 periphery was significantly reduced in both *adf4* and *ADF1-4Ri* compared with the size of those
152 in Col-0 (Fig. 1H). However, the NOR chromocenter size was not significantly altered in *adf4*
153 compared with that in Col-0, whereas a significant reduction in chromocenter size was observed
154 in *ADF1-4Ri* (Fig. 1I). This result suggests that chromocenters near the nucleoli are affected
155 differently from those near the nuclear periphery in *adf4* and *ADF1-4Ri*.
156 Subclass I *ADF*s are strongly expressed in mature leaves but less so in cotyledons (Ruzicka
157 et al. 2007). We examined the chromocenter size of both cotyledons and mature leaves (first
158 leaves) to understand the relationship between loss of subclass I *ADF* expression and
159 chromocenter size reduction. The chromocenter size in the cotyledons of *adf4* and *ADF1-4Ri*
160 was comparable to that in wild-type Col-0 (Figs. 2A–D), whereas the size of chromocenters in
161 the first leaves of *ADF1-4Ri* was significantly reduced (Figs. 2E–H), further indicating the role
162 of subclass I ADFs in the regulation of chromocenter size.
163 The reduction in chromocenter size could be caused by the decondensation of
164 chromocenters. We performed in situ fluorescence hybridization (FISH) using a probe
165 specifically labeling centromeric repetitive DNA to examine this possibility. Although most
166 FISH labeling showed a condensed pattern, several nuclei showed diffused FISH labeling (Fig.
167 S2), suggesting that the diffusion of heterochromatin caused a reduction in chromocenter size in
168 *adf4* and *ADF1-4Ri*.
169 We also noticed that a portion of the nuclei in *ADF1-4Ri* contained chromocenters that
170 tended to be clustered compared with the relatively random distribution in Col-0 nuclei (Figs.
171 S3A and S3B). We quantified this chromocenter organization by measuring the distance of the
172 two chromocenters (Fig. S3C). The median value of the distances between any closest
173 chromocenter of nuclei was lower in *ADF1-4Ri* than that in Col-0. As the number of
174 chromocenters per nucleus was unaltered in *ADF1-4Ri,* the positioning of chromocenters of
175 *ADF1-4Ri* was disturbed and more aggregated than that in Col-0.
176 Thus, nuclear organization alters in both *adf4* and *ADF1-4Ri* but more significantly in
177 *ADF1-4Ri*.
178
179 **The size of chromocenters was altered in *act7* but not in *act2/8***
180 Among the 10 *ACT* genes in the *A. thaliana* genome (McDowell et al. 1996a), *ACT2*, *-7*, and *-8*
181 are expressed in the vegetative tissues (An et al. 1996, McDowell et al. 1996b), where subclass I
182 *ADF*s are mainly expressed (Ruzicka et al. 2007). ACT2 and ACT8 are highly similar in amino
183 acid sequences and are functionally equivalent (Kandasamy et al. 2009). We reasoned that if
184 ADFs regulate nuclear organization via AFs, it is possible that *act* mutants also show alterations
185 in nuclear organization. We therefore examined the nuclear morphology of the *act2*/*act8* double
186 mutant as well as that of *act7* mutant (Figs. 3A–C).

No significant alterations were observed in the number of chromocenters per nucleus (Fig. 3D) or in the nuclear size (Fig. 3E) in *act2/8* or *act7*. We noticed that the size of chromocenters tended to be larger in *act7* (Fig. 3C) than that in Col-0 (Fig. 3A). However, quantitative analysis of chromocenter size showed no significant difference among Col-0, *act2/8*, and *act7* when all chromocenters were included for analysis (Fig. 3F). When chromocenters at the nuclear periphery and those near the nucleolus were separately analyzed, the chromocenters at the nuclear periphery were significantly larger in *act7* than those in Col-0 (Fig. 3H), whereas the chromocenters near the nucleolus were comparable among Col-0, *act2/8*, and *act7* (Fig. 3I).

These results further confirmed that actin disturbance affects the size of chromocenters, and that chromocenters near the nucleolus were regulated differently from those at the nuclear periphery.

Gene expression profile was significantly altered in both *adf4* and *ADF1-4Ri*

The altered nuclear organization in *adf4* and *ADF1-4Ri* described above may affect gene expression. To test this idea, we performed a large-scale gene expression analysis using the Arabidopsis Gene 1.0 ST array. RNA extracted from mature leaves of 4-week-old Col-0, *adf4*, and *ADF1-4Ri* was used for microarray analysis. Two independent sets of plants were sampled for biological replication. Genes that showed more than two-fold differences in expression levels were extracted. With this criterion, we found that expression of 911 genes in total was upregulated in *adf4* and *ADF1-4Ri*, and that of 907 genes in total was downregulated in *adf4* and *ADF1-4Ri* (Figs. 4A, B). Among these, expression of 137 genes was upregulated in both *adf4* and *ADF1-4Ri*, whereas that of 232 genes was downregulated in both *adf4* and *ADF1-4Ri* (Tables S1 and S2).

Gene Ontology analysis performed for these up- or downregulated genes in both *adf4* and *ADF1-4Ri* revealed enrichment of biotic-responsive genes (Fig. 4C). We also found that downregulated genes included many nucleotide-binding-leucine-rich repeat (*NLR*) genes (Table 1). NLRs function in the recognition of pathogen effectors that are delivered into plant cells. Recognition of effectors by NLRs triggers plant immunity (Pok Man Ngou et al. 2022). Misregulation of *NLR* expression can cause autoimmunity and growth defects, and the expression level of *NLR* genes is therefore maintained at a low level in uninfected plants (Fick et al. 2022). We found that the expression of 22 *NLR* genes were further downregulated in both *adf4* and *ADF1-4Ri* (Table 1). The list of downregulated *NLR*s in both *adf4* and *ADF1-4Ri* included *RPS5* (At1g12220), whose expression is reported to be downregulated in *adf4* (Porter et al. 2012). The expression of five *NLR*s were downregulated in *adf4* but not in *ADF1-4Ri*. Twenty-one *NLR*s showed reduced expression in *ADF1-4Ri* but not in *adf4* (Table 1). Upregulated *NLRs* included one *NLR* in *adf4*, and eight *NLR*s in *ADF1-4Ri*. No *NLRs* were upregulated in both *adf4* and *ADF1-4Ri* (Table 1). This result suggests that each member of subclass I ADFs contributes differently to the regulation of expression of different *NLR*s.

qRT-PCR confirmed the altered gene expression in *adf4* and *ADF1-4Ri*

227 As we only took biological duplications for microarray analysis, we verified the microarray data
228 by performing qRT-PCR for genes that are up- or downregulated in both *adf4* and *ADF1-4Ri*.
229 We selected genes for qRT-PCR analysis based on three criteria: genes whose functions have
230 been reported; genes where the expression level is sufficiently high in Col-0 (based on eFP
231 browser analysis; http://bar.utoronto.ca/efp2/Arabidopsis/Arabidopsis_eFPBrowser2.html), and
232 genes that possess specific sequences that have low homology with other genes.
233 For upregulated genes, At1g13210, At1g18710, At1g45145, At1g52000, At1g52400, and
234 At3g45860 were selected. At1g13210 encodes autoinhibited Ca^{2+}/ATPase II (ACA.l), which
235 functions as a P4-type ATPase that maintains asymmetry between the intra- and extracellular
236 lipid layers in phospholipid membrane bilayers (Axelsen et al. 2001). At1g18710 encodes MYB
237 DOMAIN PROTEIN 47 (MYB47), a member of R2R3-MYB proteins that function in plant
238 primary and secondary metabolism, cell fate determination, development, and responses to both
239 biotic and abiotic stresses (Dubos et al. 2010). *MYB47* expression is reported to be induced by
240 wounding and methyl jasmonate (MeJA) treatment (Devoto et al. 2005). At1g45145 encodes
241 thioredoxin *h5* (TRX5), a member of *h*-type thioredoxin. *A. thaliana TRX5* is required for the
242 response to victorin, an effector produced by a fungus *Cochliobolus victoriae*, which causes
243 Victoria blight of oats (Sweat and Wolpert. 2007). At1g52000, encoding a member of jacalin-
244 related lectin family (Eggermont et al. 2017), is reportedly upregulated by treatment with both
245 jasmonic acid and MeJA (Sasaki-Sekimoto et al., 2005) as well as by inoculation with fungal
246 pathogen *Fusarium oxysporum* (Zhu et al. 2013). At1g52400 encodes BETA GLUCOSIDASE
247 18 (BGLU18), a protein that localizes the endoplasmic reticulum (ER) and accumulates in ER
248 bodies (Ogasawara et al. 2009). BGLU18 is also known to mediate hydrolysis of abscisic acid
249 (ABA)-glucose ester to produce active ABA (Han et al. 2020). At3g45860 encodes CYSTEINE-
250 RICH RECEPTOR-LIKE PROTEIN KINASE 4 (CRK4). *CRK4* expression is induced by
251 salicylic acid treatment and *Pseudomonas syringae* pv. tomato DC3000 (*Pst*) infection (Chen et
252 al. 2004). Overexpression of *CRK4* induces hypersensitive cell death (Chen et al. 2004) and
253 confers resistance to the virulent bacteria *Pst* (Yeh et al. 2015). *CRK4* overexpression can
254 enhance drought tolerance (Lu et al. 2016). The upregulation of expression of these genes in *adf4*
255 and *ADF1-4Ri* was confirmed with qRT-PCR (Figs. 5A–F).
256 For downregulated genes, At1g58602, At1g58848, At1g61300, At2g05070, At2g05540,
257 and At3g26380 were examined for their expression with qRT-PCR. At1g58602, At1g58848, and
258 At1g61300 encode NLRs. NLRs can be divided into three groups according to their N-terminal
259 domains, namely, those with Toll/interleukin-1 receptor (TIR) domain, coiled-coil (CC) domain
260 (CNL), and RESISTANCE TO POWDERY MILDEW (RPW) 8-like CC domain (Pok Man
261 Ngou et al. 2022). At1g58602, At1g58848, and At1g61300 are all CNL. At1g58602 encodes
262 RPP7 (for resistance to *Peronospora paracitica* 7), which is required for resistance against
263 oomycete *Hyaloperonospora paracitica* Hiks1 (McDowell et al. 2000). The expression of
264 At1g58602, At1g58848, and At1g61300 in wild-type Col-0 was low but detectable (Figs. 5G–I).
265 However, in *adf4* and *ADF1-4Ri*, the expression of these *NLRs* was reduced to an undetectable
266 level (Figs. 5G–I), confirming the microarray results.

267 At2g05070 encodes light-harvesting chlorophyll-binding 2.2 (Lhcb2.2). *Lhcb1*, *Lhcb2*, and
268 *Lhcb3* genes encode polypeptides for trimeric LHCII (Jansson 1999). Lhcb1 is the most
269 abundant among these Lhcb proteins, and Lhcb2 plays a critical role in state transitions
270 (Pietrzykowska et al. 2014). Three genes in *A. thaliana* Col-0 encode *Lhcb2*, namely, *Lhcb2.1*
271 (At2g05100), *Lhcb2.2* (At2g05070), and *Lhcb2.3* (At3g27690). As *Lhcb2.1*, *2.2*, and *2.3* encode
272 identical proteins (Jansson 1999), we designed primers that detect the 3'-UTR of *Lhcb2.2* that
273 showed a decrease in *Lhcb2.2* expression in both *adf4* and *ADF1-4Ri* (Fig. 5J). The expression of
274 *Lhcb2.1* (At2g05100) and *Lhcb2.3* (At3g27690) also exhibited a degree of decrease in
275 expression according to microarray analysis (Table S3). At2g05540 encodes a member of
276 glycine-rich protein family, although the function is largely unknown. Expression of At2g05540
277 is regulated by SWI/SNF chromatin remodeling protein AtCHR12 (Mlynárová et al. 2007) and
278 by the SET domain protein, SDG4, which maintains the level of H3K4 and H3K36 methylation
279 (Cartagena et al. 2008). At3g26380 encodes β-$_L$-ARAPASE (APSE) that functions in the
280 hydrolysis of β-$_L$-arabinopyranosyl residues in arabinogalactan-proteins. A mutation in APSE
281 causes inhibition of the elongation growth of hypocotyls (Imaizumi et al. 2017). The expression
282 of both At2g05540 and At3g26380 was reduced in *adf4* and *ADF1-4Ri* (Figs. 5K and 5L).
283 Overall, qRT-PCR analyses confirmed the microarray results, and we concluded that expression
284 of many genes, including those encoding NLRs, was significantly altered in *adf4* and *ADF1-4Ri*.
285
286
287 **DISCUSSION**
288
289 Herein, we showed that chromocenter organization was significantly altered in both *adf4* and
290 *ADF1-4Ri*. The size of DAPI-stained chromocenters was significantly reduced in both *adf4* and
291 *ADF1-4Ri*, and part of nuclei in *ADF1-4Ri* showed clustered chromocenters. This reduction in
292 size was likely caused by the decondensation of chromocenters. In the *act7* mutant but not the
293 *act2/8* mutant, the size of chromocenters was increased compared with that of Col-0. These
294 results suggest that disturbances in AF organization and dynamics affect chromocenter
295 organization. Microarray analyses revealed alterations in the expression of many genes in *adf4*
296 and *ADF1-4Ri*. Overall, our results indicate that subclass I ADFs and ACT function in the
297 regulation of nuclear organization and gene expression.
298 Indeed, the loss of *ADF* expression in mammalian cells causes alteration in nuclear
299 organization. Mammalian genomes have three ADFs, namely, Cofilin-1 (COF), ADF, and COF-
300 2. The depletion of both COF and ADF expression induces severe deformation of nuclear shape
301 in mice (Kanellos et al. 2015) and in several mammalian cultured cells, including HeLa cells
302 (Wiggan et al. 2017). The nuclear deformation in COF/ADF-silenced cells is associated with
303 excessive activation of myosin-II in the cytoplasm and disruption of the nuclear lamina (Wiggan
304 et al. 2017). The cytoplasmic AFs are connected with the nuclear envelope-embedded linker of
305 the nucleoskeleton and cytoskeleton complex, which is composed of outer nuclear envelope-
306 localized Klarsicht, ANC-1, and SYNE homology (KASH) domain-containing nesprins and

307 inner nuclear envelope-localized SUN (Sad1 and UNC-84) domain-containing proteins (Tamura
308 et al. 2015). SUN proteins interact with nuclear lamina (Tamura et al. 2015), and nuclear lamina
309 interact with heterochromatin (Hoskins et al. 2021). Nuclei in COF/ADF-depleted mammalian
310 cells show the disorganization of the nuclear lamina (Wiggan et al. 2017), and the authors
311 concluded that excessive tension in the cytoplasm caused by the depletion of COF/ADF results
312 in alterations in nuclear organization and gene expression (Wiggan et al. 2017).
313 COF/ADF-depleted HeLa cells exhibit a significant reduction in the level of histone H3
314 trimethylated at lysine 27 (H3K27me3), which marks facultative heterochromatin and is mainly
315 localized at the nuclear periphery (Wiggan et al. 2017). This phenotype is similar to the
316 reduction in the size of chromocenters in *adf4* and *ADF1-4Ri*. In plants, DAPI-stained
317 chromocenters are colocalized with the heterochromatin mark H3K9me2 (Fransz et al. 2003). In
318 addition, chromocenters at the nuclear periphery were more strongly affected compared with
319 those near the nucleoli in *adf4* and *ADF1-4Ri* (see Figs. 1H and 1I). The clustered
320 chromocenters in *ADF1-4Ri* (Fig. S3) was similar to the polarized organization of
321 chromocenters observed in *A. thaliana* mutants of KASH and SUN (Sakamoto et al. 2022).
322 Thus, the reduction in chromocenter size and alteration in gene expression in *adf4* and *ADF1-*
323 *4Ri* could be caused by disturbed cytoplasmic AFs, similar to that in mammalian cells.
324 Chromocenters at the nuclear periphery in *act7* were also affected differently from those
325 near the nucleoli, and therefore the mechanism that caused alteration in chromocenter size in
326 *act7* could partly overlap with that in *adf4* and *ADF1-4Ri*. However, as opposed to that in *adf4*
327 and *ADF1-4Ri*, the size of the chromocenter became enlarged in *act7*, suggesting that ACT7 is
328 involved in the regulation of chromocenter organization via a different mechanism. In
329 mammalian cells, the loss of *ACTIN* expression causes altered nuclear organization and gene
330 expression. Embryonic fibroblasts of β-actin knockout mouse mutants showed an increase in
331 nuclear area and a decrease in DAPI fluorescence intensity in nuclei (Xie et al. 2018). Both
332 immunofluorescence microscopy and western blotting showed that the amount of histone H3
333 trimethylated at lysine 9 (H3K9me3), another marker of facultative heterochromatin, was
334 increased in β-actin knockout cells. Heterochromatin protein (HP)1α is a central component of
335 heterochromatin in mammalian and *Drosophila* cells (Saksouk et al. 2015). The number of
336 HP1α-labeled spot areas increased in β-actin knockout cells (Xie et al. 2018). This increase in the
337 heterochromatin area in β-actin knockout cells is similar to the increased chromocenter size in
338 *act7*.
339 In mammalian cells, β-actin is an essential component of the chromatin remodeling
340 complex BRG1/BRM-associated factor (BAF, mammalian SWI/SNF) (Kapoor and Shen 2014).
341 β-actin is required for maximum ATPase activity of Brg1, an ATPase subunit of the BAF
342 complex. Loss of β-actin significantly decreased DNA binding of Brg1 (Xie et al. 2018).
343 Therefore, β-actin regulates heterochromatin organization through its DNA-binding activity of
344 the BAF complex (Xie et al. 2018). In plants, orthologs of SWI/SNF subunits have been
345 identified, and their functions have been characterized (Reyes 2014, Nishioka et al. 2020). The
346 interaction between actin and BRM has not yet been reported in plants, but our results suggest

347 that plant actin also plays a role in regulating the activities of the chromatin remodeling complex,
348 which regulates heterochromatin organization and gene expression.
349 We showed that genes related to plant defense response are both up- and downregulated in
350 *adf4* and *ADF1-4Ri*. Furthermore, we found that expression of many *NLR* genes are
351 downregulated in *adf4* and *ADF1-4Ri*. Twenty-two *NLRs* showed reduced expression in both
352 *adf4* and *ADF1-4Ri*. While our microarray analysis used uninfected mature leaves, it has been
353 shown that *RPS5* expression, of which reduction was confirmed in our microarray, was reduced
354 both in uninfected and *Pst* AvrPphB-infected *adf4* (Porter et al. 2012), suggesting that *NLR*
355 expression is also affected in *adf4* and *ADF1-4Ri* during pathogen infection. Our result that
356 expression of some *NLRs* was suppressed only in *adf4* or in *ADF1-4Ri* suggests that different
357 ADF members affect expression of different sets of *NLR*s. This could explain previous results
358 where loss of *ADF*s results in both increase or decrease in resistance depending on pathogens
359 and that different ADF members affect pathogen response differently. Tian et al. reported that *A.*
360 *thaliana adf4* showed an increased susceptibility against the bacterial pathogen *Pst* harboring
361 AvrPphB, whereas *adf4* showed comparable susceptibility against *Pst* or *Pst* AvrB. Neither *adf1*
362 nor *adf3* showed altered susceptibility against these pathogens. The susceptibility of *ADF1-4Ri*
363 against *Pst* AvrPphB was also comparable with that of Col-0 (Tian et al. 2009). However, both
364 *adf4* and *ADF1-4Ri* showed an increased resistance to *G. orontii* (Inada et al. 2016). In wheat
365 (*Triticum aestivum* L.), the suppression of different members of ADFs has different effects on
366 immunity against fungus causing stripe rust. Wheat genotype Suwon 11 is resistance to *Puccinia*
367 *striiformis* f.sp. *tritici* CYR23 but is susceptible to *P. striiformis* f.sp. *tritici* CYR31. Knockdown
368 of *TaADF7* (Fu et al. 2014) and *TaADF4* (Zhang et al. 2017) both increased a susceptibility
369 against CYR23. By contrast, knockdown of *TaADF3* expression caused increased resistance
370 against CYR31 (Tang et al. 2016). It is possible that TaADF3, 4, and 7 affect the expression of
371 different set of *NLR*s, which results in the above-mentioned phenotypic differences.
372 Taken together, our results strongly suggests that *A. thaliana* subclass I ADFs regulate
373 various aspects of plant physiology including pathogen response through their roles in regulation
374 of nuclear organization and gene expression. Future research elucidating the mechanism how
375 ADFs and actin regulate nuclear organization and gene expression will contribute to understand
376 the new roles of plant cytoskeletons as well as new mechanisms regulating gene expression.
377
378
379 **MATERIALS AND METHODS**
380
381 **Plant materials**
382 *Arabidopsis* seeds were suspended in autoclaved 0.1% agarose and incubated at 4°C for
383 vernalization for more than 1 day (up to 2 weeks) before direct sowing on 1:3
384 metromix:vermiculite in plastic pots. Entire pots were covered with plastic wrap for 1 week after
385 sowing to maintain humidity and to encourage germination. Plants were grown at 22°C in a
386 growth chamber under a 16-h light:8-h dark photoperiod (LH-411PFD-S, NK Systems, Osaka,
387 Japan).

388
389 **Observation of chromocenters**
390 For observation of chromocenters in epidermal cells, 4 week old mature leaves were fixed with
391 3:1 ethanol:acetic acid at R.T. overnight. Fixed leaves were then rinsed with milliQ three times
392 before stained with 1 ug/mL DAPI. Images of DAPI-stained nuclei in epidermal cells were
393 excited with 405 nm laser, and fluorescence between 410-585 nm was captured using confocal
394 laser scanning microscope (Zeiss LSM700) that was equipped with ×63 objective lens (N.A.
395 1.4). Z-stack images were obtained with 0.5 μm step size.
396
397 **Quantitative image analysis of chromocenters**
398 Obtained Z-stack confocal images of DAPI were combined using maximum intensity projection.
399 To measure the heterochromatin number and size, a binary image was obtained from the
400 maximum intensity projection image by intensity thresholding. Before binarization, a Gaussian
401 filter (sigma = 2 pixels) was applied to the images in order to improve the signal to noise ratio.
402 Intensity thresholding was performed based on Yen's method (Yen et al. 1995), and then the
403 binary images were masked by manually segmented nuclear regions. Number and size of the
404 heterochromatin blobs in the binary images were measured. All image processing and analysis
405 were performed by ImageJ software (Schneider et al. 2012).
406
407 **Microarray analysis**
408 4-week old mature leaves were harvested and frozen in liquid N_2. Total RNA was extracted
409 using TRIzol reagent (Life Technologies Japan, Tokyo, Japan) and purified with an RNeasy
410 Micro kit (Qiagen) following the manufacturers' instructions. Arabidopsis Gene 1.0 ST arrays
411 (Thermo Fisher Scientific) was used for microarray analysis. Quality of RNA was checked using
412 RNA 600 Nano LabChip Kit (Agilent) following the manufacturer's protocol. Sense-strand DNA
413 target preparation was performed with WT Expression Kit (Ambion) and GeneChip WT
414 Terminal labeling Kit and Controls Kit (Thermo Fisher Scientific) following the manufacturer's
415 protocols. Hybridization, washing, and staining procedures were performed on Fluidics Station
416 450 (Affymetrix) with GeneChip Hybridization, Wash, and Stain Kit (Thermo Fisher Scientific).
417 GeneChips were scanned with GeneChip Scanner 3000 7G. Gene-level RMA sketch
418 normalization was performed was performed using standard settings for GeneChip Gene 1.0 ST
419 arrays on Expression Console Version 1.3 (Affymetrix). Microarray data were quantified using
420 Transcriptome Analysis Console 4.0 (Thermo Fisher Scientific). Expression levels were
421 compared between Col-0 and *adf4* and between Col-0 and *ADF1-4Ri* by calculating average log2
422 ratios. Significantly altered genes were defined as those with a fold change of ≥2 or ≤-2 from
423 Col-0 for both *adf4* and *ADF1-4Ri*. GO analysis was performed using PANTHER 17.0 (Released
424 20220223).
425
426 **qRT-PCR**
427 Mature leaves were harvested from 4-week-old plants and frozen in liquid N_2. Total RNA was
428 extracted using TRIzol reagent (Life Technologies Japan, Tokyo, Japan) in accordance with the

429 manufacturer's protocol. cDNA was synthesized with the ReverTra Ace qPCR RT Master Mix
430 with gDNA Remover (TOYOBO) using 100 ng of total RNA. qRT-PCR was carried out using
431 THUNDERBIRD SYBR qPCR Mix (TOYOBO) on 7300 Real Time PCR Systerm (Applied
432 Biosysterms). *ACT8* (At1g49240) was used as internal control gene for normalization. Primer
433 information is shown in Table S3.
434
435
436 **REFERENCES**
437

438 An, Y-Q., McDowell, J.M., Huang, S., McKinney, E.C., Chambliss, S., and Meagher, R.B.
439 (1996) Strong, constitutive expression of the *Arabidopsis ACT2/ACT8* actin subclass in
440 vegetative tissues. Plant J. 10, 107-121.
441 Axelsen, K.B., and Palmgren, M.G. (2001) Inventory of the superfamily of P-type ion pumps in
442 Arabidopsis. Plant Physiol. 126, 696-706.
443 Baarlink, C., Wang, H., and Grosse, R. (2013) Nuclear actin network assembly by formins
444 regulates the SRF coactivator MAL. Science 340, 864-867.
445 Burgos-Rivera, B., Ruzicka, D.R., Deal, R.B., McKinney, E.C., King-Reid, L., and Meagher,
446 R.B. (2008) *ACTIN DEPOLYMERIZING FACTOR9* controls development and gene expression
447 in *Arabidopsis*. Plant Mol Biol. 68, 619-632.
448 Cartagena, J.A., Matsunaga, S., Seki, M., Kurihara, D., Yokoyama, M., Shinozaki, K. et al.
449 (2008) The *Arabidopsis* SDG4 contributes to the regulation of pollen tube growth by methylation
450 of histone H3 lysines 4 and 36 in mature pollen. Dev. Biol. 315, 355-368.
451 Chen, K., Fan, B., Du, L., and Chen, Z. (2004) Activation of hypersensitive cell death by
452 pathogen-induced receptor-like protein kinases from *Arabidopsis*. Plant Mol. Biol. 56, 271-283.
453 Clément, M., Ketelaar, T., Rodiuc, N., Banora, M.Y., Smertenko, A., Engler, G., et al. (2009)
454 Actin-Depolymerizing Factor2-mediated actin dynamics are essential for root-knot nematode
455 infection of *Arabidopsis*. Plant Cell 21, 2963-2979.
456 Davidson, P.M., and Cadot, B. (2021) Actin on and around the nucleus. Trend. Cell Biol. 31,
457 211-223.
458 Devoto, A., Ellis, C., Magusin, A., Chang, H-S., Chilcott, C., Zhu, T., and Turner, J.G. (2005)
459 Expression profiling revelas COI1 to be a key regulator of genes involved in wound- and methyl
460 jasmonate-induced secondary metabolism, defence, and hormone interactions. Plant Mol. Biol.
461 58, 497-513.
462 Dong, C-H., Xia, G-X., Hong, Y., Ramachandran, S., Kost, B., and Chua, N-H. (2001) ADF
463 proteins are involved in the control of flowering and regulate F-actin organization, cell expansion
464 and organ growth in Arabidopsis. Plant Cell 13, 1333-1346.
465 Dubos, C., Stracke, R., Grotewold, E., Weisshaar, B., Martin C., and Lepniec, L. (2010) MYB
466 transcription factors in *Arabidopsis*. Trend. Plant Sci. 15, 573-581.
467 Eggermont, L., Verstraeten, B., and Van Damme E.J.M. (2017) Genome-wide screening for
468 lectin motifs in *Arabidopsis thaliana*. Plant Genome 10. Doi: 10.3835/plantgenome2017.02.0010

469 Fick, A., Swart, V., and van den Berg, N. (2022) The ups and downs of plant NLR expression
470 during pathogen infection. Front. Plant Sci. 13, 921148.
471 Fransz, P., de Jong, J.H., Lysak, M., Castiglione, M.R., and Schubert, I. (2002) Interphase
472 chromosomes in *Arabidopsis* are organized as well defined chromocenters from which
473 euchromatin loops emanate. Proc. Natl. Acad. Sci., U.S.A. 99, 14584-14589.
474 Fransz, P., Soppe, W., and Schubert, I. (2003) Heterochromatin in interphase nuclei in
475 *Arabidopsis thaliana*. Chrom. Res. 11, 227-240.
476 Fu, Y., Duan, X., Tang, C., Li, X., Voegele, R.T., Wang, X. et al. (2014) TaADF7, an actin-
477 depolymerizing factor, contributes to wheat resistance against *Puccinia striiformis* f.sp. *tritici*.
478 Plant J. 78, 16-30.
479 Han, Y., Watanabe, S., Shimada, H., and Sakamoto, A. (2020) Dynamics of the leaf endoplasmic
480 reticulum modulate β-glucosidase-mediated stress activated ABA production from its glucosyl
481 ester. J. Exp. Bot. 71, 2058-2071.
482 Henty, J.L., Bledsoe, S.W., Khurana, P., Meagher, R.B., Day, B., Blanchoin, L., et al. (2011)
483 Arabidopsis Actin Depolymerizing Factor 4 modulates the stochastic dynamic behavior of actin
484 filaments in the cortical array of epidermal cells. Plant Cell 23, 3711-3726.
485 Henty-Ridilla, J.L., Li, J., Blanchoin, L., and Staiger, C.J. (2013) Actin dynamics in the cortical
486 array of plant cells. Curr. Opin. Plant Biol. 16, 678-687.
487 Hoskins, V.E., Smith, K., and Reddy, K.L. (2021) The shifting shape of genomes: dynamics of
488 heterochromatin interactions at the nuclear lamina. Curr. Opin. Gene. Dev. 67, 163-173.
489 Hurst, V., Shimada, K., and Gasser, S.M. (2019) Nuclear actin and actin-binding proteins in
490 DNA repair. Trend. Cell Biol. 29, 462-476.
491 Imaizumi, C., Tomatsu, H., Kitazawa, K., Yoshimi, Y., Shibano, S., Kikuchi, K. et al. (2017)
492 Heterologous expression and characterization of an Arabidopsis β-$_L$-arabinopyranosidase and α-
493 $_D$-galactosidases acting on β-$_L$-arabinopyranosyl residues. J. Exp. Bot. 68, 4651-4661.
494 Inada, N., Higaki, T., and Hasezawa, S. (2016) Nuclear function of subclass I Actin
495 Depolymerizing Factor contributes to susceptibility in Arabidopsis to an adapted powdery
496 mildew fungus. Plant Physiol. 170, 1420-1434.
497 Inada, N. (2017) Plant Actin Depolymerizing Factor – Actin microfilament disassembly and
498 more. J. Plant Res. 130, 227-238.
499 Inada, N., Takahashi, N., and Umeda, M. (2021) Arabidopsis thaliana subclass I ACTIN
500 DEPOLYMERIZING FACTORs and vegetative ACTIN2/8 are novel regulators of
501 endoreplication. J. Plant Res. 134, 1291-1300.
502 Jansson, S. (1999) A guide to the Lhc genes and their relatives in Arabidopsis. Trend. Plant Sci.
503 4, 236-240.
504 Kandasamy, M.K., McKinney, E.C., and Meagher, R.B. (2009) A single vegetative actin
505 isovariant overexpressed under the control of multiple regulatory sequences in sufficient for
506 normal Arabidopsis development. Plant Cell 21, 701-718.
507 Kandasamy, M.K., McKinney, E.C., and Meagher, R.B. (2010) Differential sublocalization of
508 actin variants within the nucleus. Cytoskeleton 67, 729-743.

509 Kanellos, G., Zhou, J., Patel, H., Ridgway, R.A., Huels, D., Gurniak, C.B. et al. (2015) ADF and
510 Cofilin1 control actin stress fibers, nuclear integrity, and cell survival. Cell Rep. 13, 1949-1964.
511 Kapoor, P., and Shen, X. (2014) Mechanisms of nuclear actin in chromatin remodeling
512 complexes. Trend. Cell Biol. 24, 238-246.
513 Lu, K., Liang, S., Wu, Z., Bi, C., Yu, Y-T., Wang, X-F. et al. (2016) Overexpression of an
514 Arabidopsis cysteine-rich receptor-like protein kinase, CRK5, enhances abscisic acid sensitivity
515 and confers drought tolerance. J. Exp. Bot. 67, 5009-5027.
516 McDowell, J.M., Huang, S., McKinney, E.C., An, Y-Q., and Meagher, R.B. (1996a) Structure
517 and evolution of the actin gene family in *Arabidopsis thaliana*. Genetics 142, 587-602.
518 McDowell, J.M., An, Y-Q., Huang, S., McKinney, E.C., and Meagher, R.B. (1996b) The
519 Arabidopsis *ACT7* actin gene is expressed in rapidly developing tissues and responds to several
520 external stimuli. Plant Physiol. 111, 699-711.
521 McDowell, J.M., Cuzick, A., Can, C., Beynon, J., Dangl, J.L., and Holub, E.B. (2000) Downy
522 mildew (*Peronospora parasitica*) resistance genes in Arabidopsis vary in functional
523 requirements for *NDR1*, *EDS1*, *NPR1* and salicylic acid accumulation. Plant J. 22, 523-529.
524 McKinney, E.C., and Meagher, R.C. (1998) Members of the Arabidopsis actin gene family are
525 widely dispersed in the genome. Genetics 149, 663-675.
526 Mlynárová, L., Nap, L-P., and Besseling, T. (2007) The SWI/SNF chromatin-remodeling gene
527 *AtCHR12* mediates temporary growth arrest in Arabidopsis thaliana upon perceiving
528 environmental stress. Plant J. 51, 874-885.
529 Mondal, H.A., Louis, J., Archer, L., Patel, M., Nalam, V.J., Sivapalan, V., et al. (2018)
530 Arabidopsis *ACTIN-DEPOLYMERIZING FACTOR3* is required for controlling aphid feeding
531 from the phloem. Plant Physiol.176, 879-890.
532 Nishioka, S., Sakamoto, T., and Matsunaga, S. (2020) Role of BRAHMA and its interacting
533 partners in plant chromatin remodeling. Cytologia 85, 263-267.
534 Ogasawara, K., Yamada, K., Christeller, J.T., Kondo, M., Hatsugai, N., Hara-Nishimura, I. et al.
535 (2009) Constitutive and inducible ER bodies of *Arabidopsis thaliana* accumulate distinct β-
536 glucosidases. Plant Cell Physiol. 50, 480-488.
537 Ortega-Ortega, Y., Carrasco-Castilla, J., Juárez-Verdayes, M.A., Toscano-Morales, R., Fonseca-
538 García, C., Nava, N., et al. (2020) Actin Depolymerizing Factor modulates rhizobial infection
539 and nodule organogenesis in common bean. Int. J. Mol. Sci. 21, 1970.
540 Percipalle, P., and Vartiainen, M. (2019) Cytoskeletal proteins in the cell nucleus: a special
541 nuclear actin perspective. Mol. Biol. Cell 30, 1781-1785.
542 Pietrzykowska, M., Suorsa, M., Semchonok, D.A., Tikkanen, M., Boekema, E.J., Aro, E-M., et
543 al. (2014) The light-harvesting chrolophyll *a/b* binding proteins Lhcb1 and Lhcb2 play
544 complementary roles during state transitions in *Arabidopsis*. Plant Cell 26, 3646-3660.
545 Pok Man Ngou, B., Ding, P., and Jones, J.D.G. (2022) Thirty years of resistance : Zig-zag
546 through the plant immune system. Plant Cell 34, 1447-1478.
547 Pontvianne, F.,and Grob, S. (2020) Three-dimensional nuclear organization in *Arabidopsis*
548 *thaliana*. J. Plant Res. 133, 479-488.

549 Porter, K., and Day, B. (2013) Actin branches out to link pathogen preception and host gene
550 regulation. Plant Sign. Behav. 8, e23468.
551 Porter, K., and Day, B. (2016) From filaments to function: the role of the plant actin cytoskeleton
552 in pathogen perception, signaling and immunity. J. Intergr. Plant Biol. 58, 299-311.
553 Porter, K., Shimono, M., Tian, M., and Day, B. (2012) Arabidopsis Actin-Depolymerizing
554 Factor-4 links pathogen perception, defense activation and transcription to cytoskeletal
555 dynamics. PLOS Pathogens 8, e1003006.
556 Qian, D., Zhang, Z., He, J., Zhang, P., Ou, X., Li, T., et al. (2019) Arabidopsis ADF5 promotes
557 stomatal closure by regulating actin cytoskeleton remodeling in response to ABA and drought
558 stress. J. Exp. Bot. 70, 435-446.
559 Reyes, J.C. (2014) The many faces of plant SWI/SNF complex. Mol. Plant 7, 454-458.
560 Ruzicka, D.R., Kandasamy, M.K., McKinney, E.C., Burgos-Rivera, B., and Meagher, R.B.
561 (2007) The ancient subclasses of Arabidopsis ACTIN DEPOLYMERIZING FACTOR genes
562 exhibit novel and differential expression. Plant J. 52, 460-472.
563 Sakamoto, T., Sakamoto, Y., Grob, S., Slane, D., Yamashita, T., Ito, N. et al. (2022) Two-step
564 regulation of centromere distribution by condensin II and the nuclear envelope proteins. Nat.
565 Plants 8, 940-953.
566 Saksouk, N., Simboeck, E., and Déjardin, J. (2015) Constitutive heterochromatin formation and
567 transcription in mammals. Epigene. Chrom. 8, 3.
568 Sasaki-Sekimoto, Y., Taki, N., Obayashi, T., Aono, M., Matsumoto, F., Sakurai, N. et al. (2005)
569 Coodinated activation of metabolic pathways for antioxidants and defence compounds by
570 jasmonates and their roles in stress tolerance in Arabidopsis. Plant J. 44, 653-668.
571 Schneider, C.A., Rasband, W.S., and Eliceiri, K.W. (2012) NIH Image to ImageJ: 25 years of
572 image analysis. Nat. Methods 9, 671–675. doi:10.1038/nmeth.2089
573 Sengupta, S., Mangu, V., Sanchez, L., Bedre, R., Joshi, R., Rajasekaran, K., et al. (2019) An
574 actin-depolymerizing factor from the halophyte smooth cordgrass, *Spartina alterniflora*
575 (SaADF2), is superior to its rice homolog (OsADF2) in conferring drought and salt tolerance
576 when constitutively overexpressed in rice. Plant Biotech. J. 17, 188-205.
577 Sun, Y., Zhong, M., Li, Y., Zhang, R., Su, L., Xia, G., et al. (2021) *GhADF6*-mediated actin
578 reorganization is associated with defence against *Verticillium dahliae* infection in cotton. Mol.
579 Plant Pathol. 22, 1656-1667.
580 Sweat, T.A., and Wolpert, T.J. (2007) Thioredoxin *h5* is required for victorin sensitivity
581 mediated by a CC-NBS-LRR gene in *Arabidopsis*. Plant Cell 19, 673-687.
582 Takemoto, D., Jones, D.A., and Hardham, A.R. (2003) GFP-tagging of cell components reveals
583 the dynamics of subcellular re-organization in response to infection of *Arabidopsis* by oomycete
584 pathogens. Plant J. 33, 775-792.
585 Tamura, K., Goto, C., and Hara-Nishimura, I. (2015) Recent advances in understanding plant
586 nuclear envelope proteins involved in nuclear morphology. J. Exp. Bot. 66, 1641-1647.

587 Tang, C., Deng, L., Chen, S., Wang, X., and Kang, Z. (2016) TaADF3, an Actin-Depolymerizing
588 Factor, negatively modulates wheat resistance against *Puccinia striiformis.* Front. Plant Sci. 6,
589 1214.
590 Tian, M., Chaudhry, F., Ruzicka, D.R., Meagher, R.B., Staiger, C.J., and Day, B. (2009)
591 Arabidopsis Actin-Depolymerizing Factor AtADF4 mediates defense signal transduction
592 triggered by the *Pseudomonas syringae* effector AvrPphB. Plant Physiol. 150, 815-824.
593 Xie, X., Almuzzaini, B., Drou, N., Kremb, S., Yousif, A., Farrants, A-K.Ö., et al. (2018) β-
594 Actin-dependent global chromatin organization and gene expression programs control cellular
595 identity. FASEB J. 32, 1296-1314.
596 Xu, K., Zhao, Y., Zhao, S., Liu, H., Wang, W., Zhang, S., and Yang, X. (2021) Genome-wide
597 identification and low temperature responsive pattern of actin depolymerizing factor (ADF) gene
598 family in wheat (*Triticum aestivum* L.). Front. Plant Sci. 12, 618984.
599 Yeh, Y-H., Chang, Y-H., Huang, P-Y., Huang, J-B., and Zimmerli, L. (2015) Enhanced
600 Arabidopsis pattern-triggered immunity by overexpression of cysteine-rich receptor-like kinases.
601 Front. Plant Sci. 6, 322.
602 Yen, J.C., Chang, F.J., and Chang, S. (1995) A new criterion for automatic multilevel
603 thresholding. IEEE Trans. on Image Processing 4, 370-378.
604 Wang, L., Qiu, T., Yue, J., Guo, N., He, Y., Han, Y., et al. (2021) *Arabidopsis ADF1* is regulated
605 by MYB73 and is involved in response to salt stress affecting actin filament organization. Plant
606 Cell Physiol. 62, 1387-1395.
607 Wiggan, O., Chroder, B., Krapf, D., Bamburg, J.R., and DeLuca, J.G. (2017) Cofilin regulates
608 nuclear architecture through a myosin-II dependent mechanotransduction module. Sci. Rep. 7,
609 40953.
610 Zhang, B., Hua, Y., Wang, J., Huo, Y., Shimono, M., Day, M., et al. (2017) *TaADF4*, an actin-
611 depolymerizing factor from wheat, is required for resistance to the stripe rust pathogen *Puccinia*
612 *striiformis* f. sp. *tritici*. Plant J. 89, 1210-1224.
613 Zhu, Q-H., Stephen, S., Kazan, K., Jin, G., Fan, L., Taylor, J. et al. (2013) Characterization of
614 the defense transcriptome responsive to *Fusarium oxysporum*-infection in *Arabidopsis* using
615 RNA-seq. Gene 512, 259-266.
616
617
618

619 **Table 1.** A list of *NLR* genes that differently expressed in *adf4* and *ADF1-4Ri*.

	Upregulated	Downregulated
in *adf4* only	AT5G47280	AT1G33560
		AT1G58400
		AT1G66090
		AT1G72890
		AT5G05400
in *ADF1-4Ri* only	AT1G57650	AT3G44400
	AT1G72900	AT3G44480
	AT4G16960	AT3G44670
	AT5G04720	AT4G16860
	AT5G18360	AT4G16930
	AT5G45440	AT4G19500
	AT5G46490	AT4G19510
	AT5G47260	AT4G19520
		AT4G19530
		AT4G27220
		AT5G17880
		AT5G17890
		AT5G36930
		AT5G41740
		AT5G41750
		AT5G43725
		AT5G43740
		AT5G45230
		AT5G45490
		AT5G48620
		AT5G51630
in both *adf4* and *ADF1-4Ri*		AT1G12220
		AT1G15890
		AT1G56520
		AT1G58602
		AT1G58807
		AT1G58848
		AT1G59124

AT1G59218
AT1G61180
AT1G61190
AT1G61300
AT1G61310
AT1G62630
AT1G63350
AT1G63860
AT1G63880
AT1G72840
AT1G72850
AT1G72852
AT1G72910
AT1G72920
AT1G72930

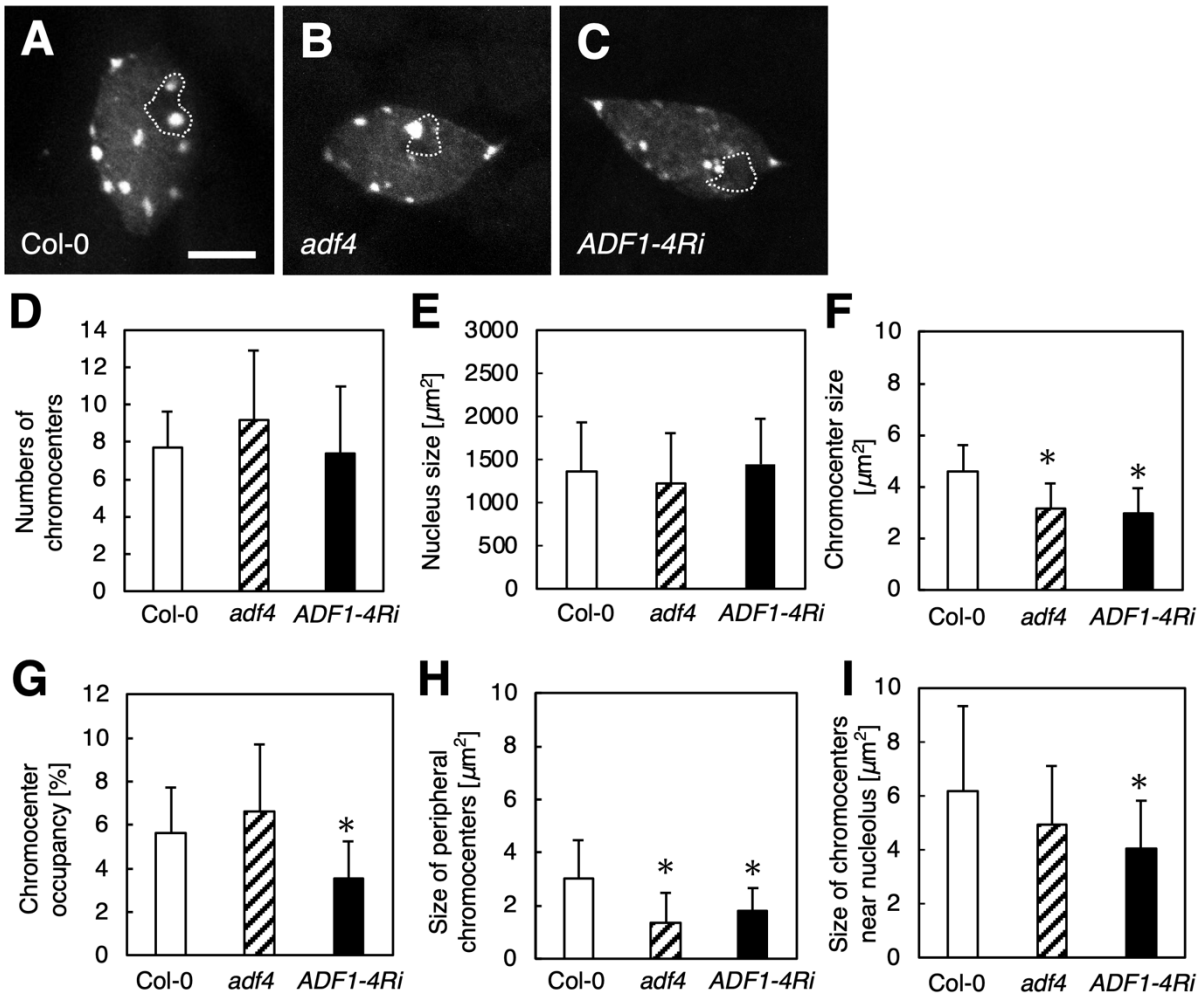

Figure 1. The size of chromocenters was reduced in *adf4* and *ADF1-4Ri* mature leaves. The fluorescence micrographs of DAPI-stained nuclei in epidermal cells of mature leaves in Col-0 (**A**), *adf4* (**B**), and *ADF1-4Ri* (**C**). Dotted lines indicate nucleoli. Bar indicates 5 µm. (**D**) Numbers of chromocenters, (**E**) the size of nuclei, (**F**) the size of chromocenters, (**G**) the percentage of chromocenter area in nuclei, (**H**) the size of chromocenters located at the nuclear periphery, and (**I**) the size of chromocenters located near the nucleoli in Col-0, *adf4*, and *ADF1-4Ri* were quantified using fluorescence micrographs. Comparison with Col-0 was performed by Student's *t*-test. Asterisks indicate that there is a significant difference (* $P<0.05$).

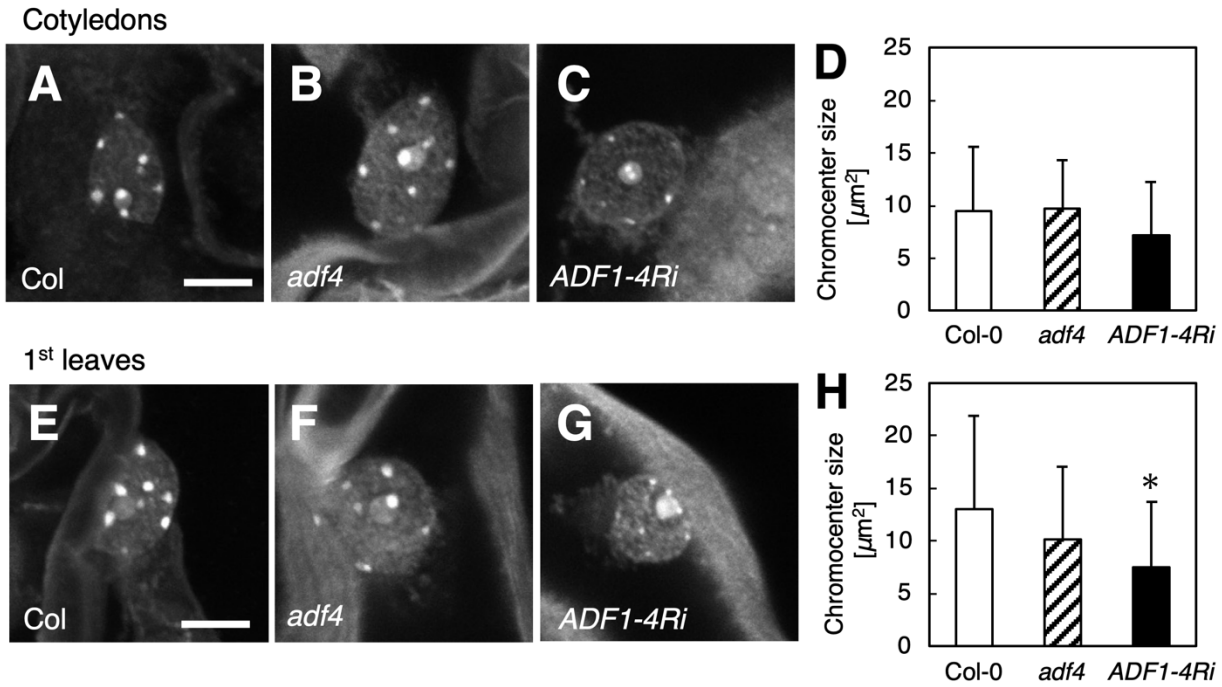

Figure 2. The size of chromocenters was less affected in cotyledons of *adf4* and *ADF1-4Ri*. The fluorescence micrographs of DAPI-stained nuclei in epidermal cells of cotyledons in Col-0 (**A**), *adf4* (**B**), and *ADF1-4Ri* (**C**). (**D**) The size of chromocenters in Col-0, *adf4*, and *ADF1-4Ri* cotyledons. The fluorescence micrographs of DAPI-stained nuclei in epidermal cells of 1st leaves in Col-0 (**E**), *adf4* (**F**), and *ADF1-4Ri* (**G**). (**H**) The size of chromocenters in Col-0, *adf4*, and *ADF1-4Ri* 1st leaves. Bars indicate 5 μm. Comparison with Col-0 was performed by Student's *t*-test. Asterisks indicate that there is a significant difference (* $P<0.05$).

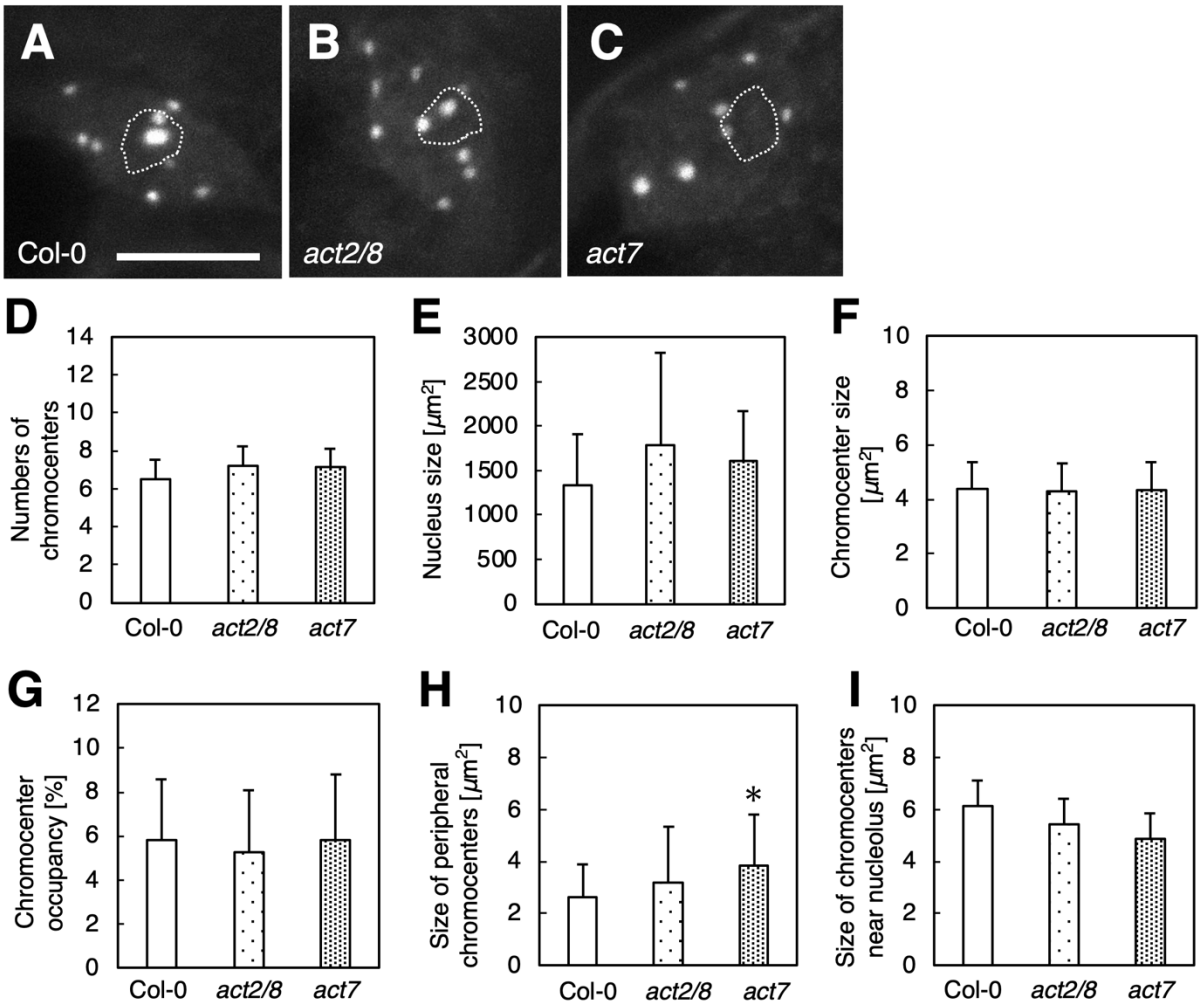

Figure 3. The size of chromocenters was increased in *act7* mature leaves. The fluorescence micrographs of DAPI-stained nuclei in epidermal cells of mature leaves in Col-0 (**A**), *act2/8* (**B**), and *act7* (**C**). Dotted lines indicate nucleoli. Bar indicates 5 µm. (**D**) Numbers of chromocenters, (**E**) the size of nuclei, (**F**) the size of chromocenters, (**G**) the percentage of chromocenter area in nuclei, (**H**) the size of chromocenters located at the nuclear periphery, and (I) the size of chromocenters located near the nucleoli in Col-0, *act2/8*, and *act7* were quantified using fluorescence micrographs. Comparison with Col-0 was performed by Student's *t*-test. Asterisks indicate that there is a significant difference (* $P<0.05$).

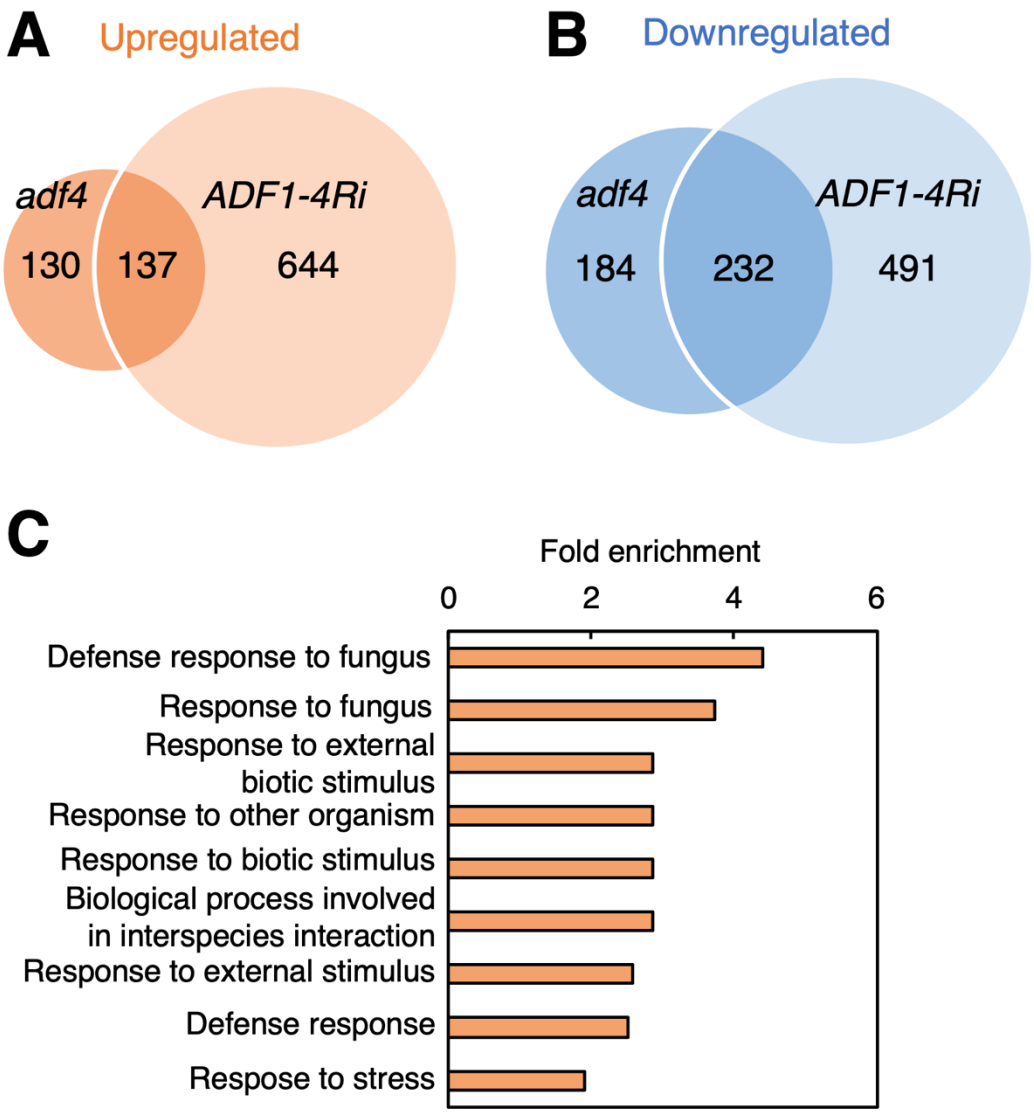

Figure 4. Microarray analysis showed altered expressions of many genes in *adf4* and *ADF1-4Ri* mature leaves. Venn diagrams of upregulated (**A**) and downregulated (**B**) genes in *adf4* and *ADF1-4Ri*. (**C**) GO analysis for genes that showed altered expression in both *adf4* and *ADF1-4Ri* (genes including both upregulated and downregulated genes).

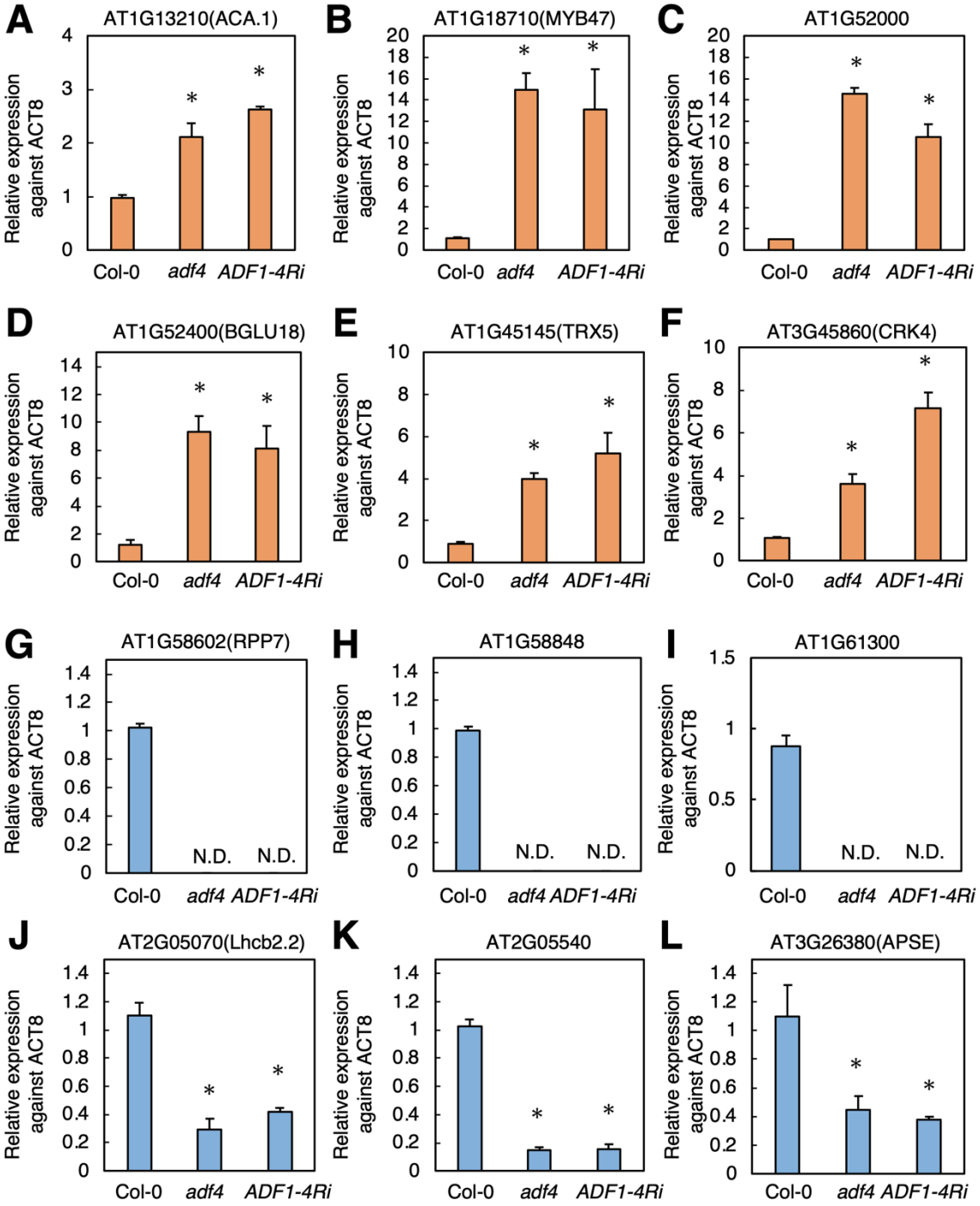

Figure 5. qRT-PCR confirmed alteration in gene expression in *adf4* and *ADF1-4Ri* shown by microarray analysis. The expressions of At1g13210 (**A**), At1g18710 (**B**), At1g52000 (**C**), At1g52400 (**D**), At1g45145 (**E**), and At3g45860 (**F**) were upregulated in both *adf4* and *ADF1-4Ri*. The expression of At1g58602 (**G**), At1g58848 (**H**), At1g61300 (**I**), At2g05070 (**J**), At2g05540(**K**), and At3g26380 (**L**) were downregulated in both *adf4* and *ADF1-4Ri*.

672 Comparison with Col-0 was performed by Student's *t*-test. Asterisks indicate that there is a
673 significant difference (* $P<0.05$).
674